

# Strategy to Extract Kitaev Interaction using Symmetry in Honeycomb Mott Insulators

Jiefu Cen<sup>1</sup> and Hae-Young Kee<sup>1,2,\*</sup>

<sup>1</sup>*Department of Physics, University of Toronto, Ontario, Canada M5S 1A7*

<sup>2</sup>*Canadian Institute for Advanced Research,  
CIFAR Program in Quantum Materials,  
Toronto, Ontario, Canada, M5G 1M1*

(Dated: March 15, 2022)

arXiv:2203.06193v1 [cond-mat.str-el] 11 Mar 2022

The Kitaev spin liquid, a ground state of the bond-dependent Kitaev model in a honeycomb lattice has been a centre of attraction, since a microscopic theory to realize such interaction in solid-state materials was discovered. A challenge in real materials though is the presence of the Heisenberg and another bond-dependent Gamma interactions detrimental to the Kitaev spin liquid, and there has been much debate on their relative strengths. Here we offer a strategy to extract the Kitaev interaction out of a full microscopic model by utilizing the symmetries of the Hamiltonian. Two tilted magnetic field directions above and below the plane related by a two-fold rotational symmetry generate distinct spin excitations originated from a specific combination of the Kitaev and Gamma interactions. Together with the in- and out-of-plane magnetic anisotropy, one can determine the Kitaev and Gamma interactions separately. Dynamic spin structure factors obtained by exact diagonalization are presented to motivate future experiments that probe spin excitations such as angle-dependent ferromagnetic resonance and inelastic neutron scattering spectroscopy. The proposed setups will advance the search for Kitaev materials.

## INTRODUCTION

An electron's orbital motion in an atom generates a magnetic field which influences its spin moment, known as spin-orbit coupling. When the coupling is strong in heavy atoms, the effective Hamiltonian is described by the spin-orbit-entangled pseudospin wave-function and the interactions among magnetic ions are highly anisotropic different from the standard Heisenberg interaction<sup>1-6</sup>. A fascinating example is the Kitaev model with a bond-dependent interaction in a two-dimensional honeycomb lattice, whose ground state is a quantum spin liquid (QSL) with Majorana fermions and  $Z_2$  vortex excitations<sup>7</sup>. There have been extensive studies on the model because in the Kitaev QSL non-Abelian excitations emerge under a magnetic field, and their braidings provide topological computation. Since a microscopic mechanism to generate such an interaction was uncovered<sup>8</sup>, intense efforts toward finding QSLs including a variety of candidate materials from spin  $S = 1/2$ <sup>9-18</sup> to higher-spin  $S$  systems have been made<sup>19-22</sup>. Despite such efforts, a confirmed Kitaev QSL is still missing.

One challenge in finding the Kitaev QSL in magnetic materials is the presence of other spin interactions which may generate magnetic orderings or other disordered phases<sup>23-29</sup>.

A generic nearest neighbour (n.n.) model in an ideal honeycomb was derived which revealed the isotropic Heisenberg and another bond-dependent interaction named the Gamma ( $\Gamma$ )<sup>25</sup>. Furthermore, there exist further neighbour interactions such as second and third n.n. Heisenberg interactions, which makes it difficult to single out the Kitaev interaction itself. There has been much debate on the relative strengths especially between the dominant Kitaev and Gamma interactions in Kitaev candidate materials<sup>13,18,28,30</sup>, and an experimental guide on how to extract the Kitaev interaction out of a full Hamiltonian is highly desirable.

In this work, we present a symmetry-based experimental strategy to determine the Kitaev interaction. Our proposal is based on the  $\pi$ -rotation around the  $a$ -axis perpendicular to one of bonds in the honeycomb plane, denoted by  $C_{2a}$  symmetry that is broken by a specific combination of the Kitaev and  $\Gamma$  interactions. This broken  $C_{2a}$  can be easily detected with the help of a magnetic field applied within the  $a - c$  plane where the  $c$ -axis is perpendicular to the honeycomb plane; spin excitations under the two field angles of  $\theta$  and  $-\theta$ , measured away from the honeycomb plane as shown in Fig. 1(a), are distinct due to the combination of the Kitaev and Gamma interactions. The two field angles are related by the  $\pi$ -rotation around  $a$ -axis, i.e.  $C_{2a}$  operation. Such differences are based on the symmetry, and signal the relative strengths of these interactions. A magnetic ordering that further enhances the broken  $C_{2a}$  symmetry does not alter the asymmetry, but quantifying the interaction strengths requires the size of magnetic ordering. For this reason, a polarized state in the high-field region would be ideal for our purpose.

To determine each of the interactions, one needs to use the conventional in- vs. out-of-plane anisotropy in spin excitations. We note that the Gamma interaction affects the conventional anisotropy, but the Kitaev does not when the field is large enough to compensate the order by disorder effect<sup>31</sup>. Thus subtracting the Gamma contribution deduced from the conventional anisotropy allows us to estimate the Kitaev interaction from the measured spin excitations under the field angles of  $\theta$  and  $-\theta$ . Both the conventional anisotropy and the  $\pi$ -rotation-related spin excitations can be measured by angle-dependent ferromagnetic resonance (FMR) or inelastic neutron scattering (INS) techniques while sweeping the magnetic field directions in the  $a - c$  plane containing the  $C_{2a}$  rotation axis.

Below we present the microscopic model and main results based on the  $\pi$ -rotation symmetry around  $a$ -axis. To demonstrate our theory, we also show the FMR and dynamical spin structure factors (DSSF) obtained by exact diagonalization (ED). We analyze the different

spin excitations under the two field angles at finite momenta using the linear spin wave theory (LSWT), which further confirms our results based on the symmetry argument. Our results will guide a future search of Kitaev materials.

## RESULT

**Model** – The generic spin exchange Hamiltonian among magnetic sites with strong spin-orbit coupling for the ideal edge sharing octahedra environment in the octahedral  $\mathbf{x} - \mathbf{y} - \mathbf{z}$  axes shown in Fig. 1(a) contains the Kitaev ( $K$ ), Gamma ( $\Gamma$ ), and Heisenberg ( $J$ ) interactions<sup>25</sup>:

$$\mathcal{H} = \sum_{\langle ij \rangle \in \alpha\beta(\gamma)} \left[ J \mathbf{S}_i \cdot \mathbf{S}_j + K S_i^\gamma S_j^\gamma + \Gamma (S_i^\alpha S_j^\beta + S_i^\beta S_j^\alpha) \right], \quad (1)$$

where  $\mathbf{S} = \frac{1}{2} \vec{\sigma}$  with  $\hbar \equiv 1$  and  $\vec{\sigma}$  is Pauli matrix,  $\langle ij \rangle$  denotes the nearest neighbor (n.n.) magnetic sites, and  $\alpha\beta(\gamma)$  denotes the  $\gamma$  bond taking the  $\alpha$  and  $\beta$  spin components ( $\alpha, \beta, \gamma \in \{x, y, z\}$ ). The x-, y-, and z-bonds are shown in red, blue, and green colours, respectively in Fig. 1(a). Further neighbour interactions and trigonal-distortion allowed interactions, and their effects will be discussed later.

To analyze the symmetry of the Hamiltonian, we rewrite the model in the  $\mathbf{a} - \mathbf{b} - \mathbf{c}$  axes<sup>32,33</sup>:

$$\begin{aligned} \mathcal{H} = \sum_{\langle i,j \rangle} & \left[ J_X (S_i^a S_j^a + S_i^b S_j^b) + J_Z S_i^c S_j^c \right. \\ & + J_{ab} [\cos \phi_\gamma (S_i^a S_j^a - S_i^b S_j^b) - \sin \phi_\gamma (S_i^a S_j^b + S_i^b S_j^a)] \\ & \left. - \sqrt{2} J_{ac} [\cos \phi_\gamma (S_i^a S_j^c + S_i^c S_j^a) + \sin \phi_\gamma (S_i^b S_j^c + S_i^c S_j^b)] \right], \end{aligned} \quad (2)$$

where  $\phi_\gamma = 0, \frac{2\pi}{3}$ , and  $\frac{4\pi}{3}$  for  $\gamma = z$ -, x-, and y-bond respectively, and the exchange interactions are given by

$$\begin{aligned} J_X &= J + J_{ac}, \quad J_Z = J + J_{ab}, \\ J_{ab} &= \frac{1}{3}K + \frac{2}{3}\Gamma, \quad J_{ac} = \frac{1}{3}K - \frac{1}{3}\Gamma. \end{aligned} \quad (3)$$

The Hamiltonian  $\mathcal{H}$  is invariant under  $\pi$ -rotation around the b-axis denoted by  $C_{2b}$  and  $\frac{2\pi}{3}$ -rotation around the c-axis by  $C_{3c}$  in addition to the inversion and time-reversal symmetry.

Our proposed experimental design is based on the observation that the  $\mathcal{H}$  is *not* invariant under  $\pi$ -rotation about the a-axis  $C_{2a}$  due to the presence of only  $J_{ac}$ , i.e., if  $J_{ac} = 0$ ,  $C_{2a}$  is also a symmetry of  $\mathcal{H}$ . Since the  $C_{2a}$  is broken by  $J_{ac}$ , if there is a way to detect the broken  $C_{2a}$ , that will signal the strength of  $J_{ac}$ . We note that the magnetic field sweeping from the c-axis to a-axis within the  $a - c$ -plane does the job. The fields with angles of  $\theta$  (blue line) and  $-\theta$  (red line) for  $0 < \theta < \frac{\pi}{2}$  shown in Fig. 1 (b) and (c) are related by  $C_{2a}$  rotation, and thus measuring the spin excitation difference between these two field directions will detect the strength of  $J_{ac}$ .

To prove our symmetry argument, we consider a full model with a magnetic field. Under a magnetic field, the total Hamiltonian including the Zeeman term is given by

$$\mathcal{H}_{\text{tot}} = \mathcal{H} + \mathcal{H}_B = \mathcal{H} - g \mu_B \sum_i \vec{S}_i \cdot \vec{h}, \quad (4)$$

where the external field  $\vec{h}$  has the polar angle  $\theta$  measured away from the  $a - b$  honeycomb plane and the azimuthal angle  $\phi$  from the a-axis as shown in Fig.1(b). The magnetic anisotropy in the spin excitation energies is defined as  $\omega_n(\theta) = E_n(\theta) - E_0(\theta)$ , where  $E_n$  and  $E_0$  are the excited and ground state energy respectively. This anisotropy is affected by all interactions other than the isotropic Heisenberg limit ( $J_X = J_Z$ ), making it difficult to quantify the effect of individual interactions. However, if we compare the two excitation anisotropies,  $\omega_n(\theta)$  and  $\omega_n(-\theta)$  for a given strength  $h$  and  $\phi = 0$  as shown in Fig. 1(c), related by  $C_{2a}$  symmetry transformation, we can eliminate the effects of all other interactions except  $J_{ac}$  thanks to symmetries of the model. Since our theory relies on the symmetry of the Hamiltonian, the ground state should break the  $C_{2a}$  symmetry only explicitly from the  $J_{ac}$  term. The magnetic field also contributes to the  $C_{2a}$  breaking, but by comparing two angles of  $\theta$  and  $-\theta$ , the effect of  $J_{ac}$  is isolated.

We focus on the lowest energy excitation  $n = 1$  which gives a dominant resonance at low temperatures, and drop the  $n$  in  $\omega_n$  from now on for simplicity, even though our proposal works for all  $n$ . We define the excitation anisotropy between the magnetic field with angles of  $\theta$  and  $-\theta$  as  $\delta\omega_K(\theta) \equiv \omega(\theta) - \omega(-\theta)$  for  $0 < \theta < \frac{\pi}{2}$ , and the conventional anisotropy between in- and out-of-plane fields as  $\delta\omega_A \equiv \omega(\theta = 0) - \omega(\theta = \frac{\pi}{2})$ . Below we first show how  $\delta\omega_K$  arises from  $J_{ac}$  under the field in the  $a - c$  plane based on the symmetry.

**Symmetry Analysis** – To understand the origin of a finite  $\delta\omega_K$  for  $\phi = 0$  under the magnetic field sweep, we first begin with a special case when  $\phi = \frac{\pi}{2}$ , i.e, when the external

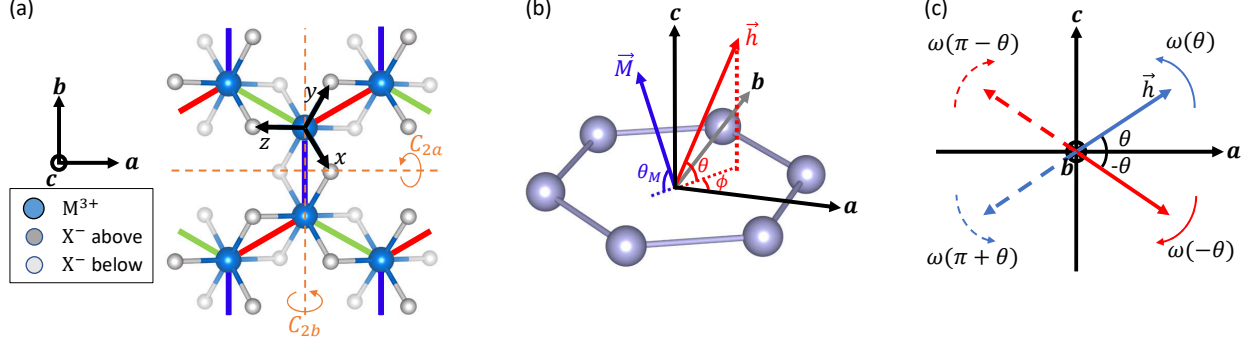


FIG. 1. (a) Schematic of the honeycomb lattice of transition metal ions (light blue) in edge sharing octahedra environment of anions (above the honeycomb plane: gray, below the plane: light gray). Octahedral  $xyz$  axes,  $abc$  axes, and the Kitaev bonds  $x$  (red),  $y$  (green),  $z$  (blue) are indicated.  $C_{2a}$  and  $C_{2b}$  symmetries (orange) are highlighted. The octahedra environment breaks  $C_{2a}$ , while  $C_{2b}$  symmetry is intact. (b) Direction of the external magnetic field in  $abc$  axes where  $\theta$  is measured from the  $a-b$  plane, and  $\phi$  is from the  $a$ -axis. The blue arrow represents the magnetic moment direction with the angle  $\theta_M$ . (c)  $\delta\omega_K(\theta)$  in the  $a-c$  plane is the difference between  $\omega(\theta)$  (blue) and  $\omega(-\theta)$  (red).  $C_{2b}$  maps  $\omega(\theta)$  to  $\omega(\pi+\theta)$ , so  $\delta\omega_K(\pi-\theta) = -\delta\omega_K(\theta)$ .

field is in the  $b-c$  plane. This is a special case where  $\delta\omega_K = 0$  for the following reason.

The Zeeman terms due to the field with the angle  $\theta$  and with  $-\theta$  are related by a  $\pi$  rotation of the field about the  $\hat{b}$  axis, denoted by

$$C_{2b,\theta} : \mathcal{H}_B \propto (\cos \theta S_i^b + \sin \theta S_i^c) \longrightarrow (\cos \theta S_i^b - \sin \theta S_i^c). \quad (5)$$

The same can be achieved by a  $\pi$ -rotation of the lattice,

$$C_{2b} : (S^a, S^b, S^c) \rightarrow (-S^a, S^b, -S^c) \text{ and } \phi_x \leftrightarrow \phi_y, \quad (6)$$

which also indicates  $\mathcal{H}$  is invariant under  $C_{2b}$ . While  $\mathcal{H}_B$  breaks the  $C_{2b}$  symmetry of  $\mathcal{H}$ , the total Hamiltonian  $\mathcal{H} + \mathcal{H}_B(\theta)$  and  $\mathcal{H} + \mathcal{H}_B(-\theta)$  are related by  $C_{2b}$  and therefore, share the same eigenenergies, i.e.,  $\delta\omega_K = 0$ . The difference due to the field is simply removed by a  $\pi$  rotation of the eigenstates about the  $\hat{b}$  axis. The magnetic field sweeping from  $\theta$  to  $-\theta$  in the other planes equivalent to  $b-c$  plane by  $C_{3c}$  symmetry also gives  $\delta\omega_K = 0$ .

Now let us consider when the magnetic field sweeps in the  $a-c$  plane. Similarly, the magnetic field directions  $\theta$  and  $-\theta$  are related by

$$C_{2a,\theta} : \mathcal{H}_B \propto (\cos \theta S_i^a + \sin \theta S_i^c) \longrightarrow (\cos \theta S_i^a - \sin \theta S_i^c). \quad (7)$$

Considering a  $\pi$  rotation of the lattice about the  $\hat{a}$  axis,

$$C_{2a} : (S^a, S^b, S^c) \rightarrow (S^a, -S^b, -S^c) \text{ and } \phi_x \leftrightarrow \phi_y, \quad (8)$$

we find  $J_X, J_Z, J_{ab}$ , terms are invariant under  $C_{2a}$ , while the  $J_{ac}$  terms transform as

$$C_{2a} : J_{ac} \rightarrow -J_{ac}. \quad (9)$$

By the same argument, if  $J_{ac} = 0$ ,  $\mathcal{H}$  is invariant under  $C_{2a}$ , and the eigenenergies of the total Hamiltonian for  $\theta$  and  $-\theta$  are the same, i.e.,  $\delta\omega_K = 0$ . If  $J_{ac} \neq 0$ , the total Hamiltonian  $\mathcal{H} + \mathcal{H}_B(\theta)$  and  $\mathcal{H} + \mathcal{H}_B(-\theta)$  cannot be related by  $C_{2a}$ , and therefore,  $\delta\omega_K \neq 0$ . We need to change the sign of  $J_{ac}$  for the  $C_{2a}$  relation to hold, i.e., the transformation of the external field angles of  $\theta$  to  $-\theta$  is equivalent to the change of  $J_{ac}$  to  $-J_{ac}$ . Thus, the lack of  $C_{2a}$  symmetry allows us to single out the  $J_{ac}$  interaction through  $\delta\omega_K$ .

Since  $J_{ac}$  contains a combination of the Kitaev and  $\Gamma$  interactions, we need other methods to subtract the  $\Gamma$  contribution. The in- and out-of-plane anisotropy,  $\delta\omega_A$  offers precisely the other information. We note that the in- and out-of-plane anisotropy  $\delta\omega_A$  is determined by  $J_Z - J_X = \Gamma$ . Thus, for the ideal edge sharing octahedral environment, we can first estimate  $\Gamma$  from the measured  $\delta\omega_A$ , and then extract the Kitaev strength by subtracting the  $\Gamma$  contribution from the measured  $\delta\omega_K(\theta)$ .

Below we show numerical results of spin excitations obtained by ED on a 24-site cluster which can be measured by angle-dependent FMR and INS techniques under magnetic field angles of  $\theta$  and  $-\theta$  with  $\phi = 0$ .

**Angle-Dependent Ferromagnetic Resonance** – FMR is a powerful probe to study ferromagnetic or spin correlated materials. FMR spectrometers record the radio-frequency (RF) electromagnetic wave that is absorbed by the sample of interest placed under an external magnetic field. To observe the resonance signal, the resonant frequency of the sample is changed to match that of the RF wave under a scan of the external magnetic field, so the excitation anisotropy  $\delta\omega(\theta)$  leads to the anisotropy in the resonant magnetic field. FMR provides highly resolved spectra over a large energy range and has been used to investigate exchange couplings<sup>34–37</sup> and anisotropies<sup>38,39</sup> due to its dependence on the magnetic field angle. Here, for simplicity, we calculate the excitation energy probed by the RF field (details can be found in the Methods) with a set magnetic field strength for spin  $\frac{1}{2}$  using ED on a  $C_3$ -symmetric 24-site cluster.

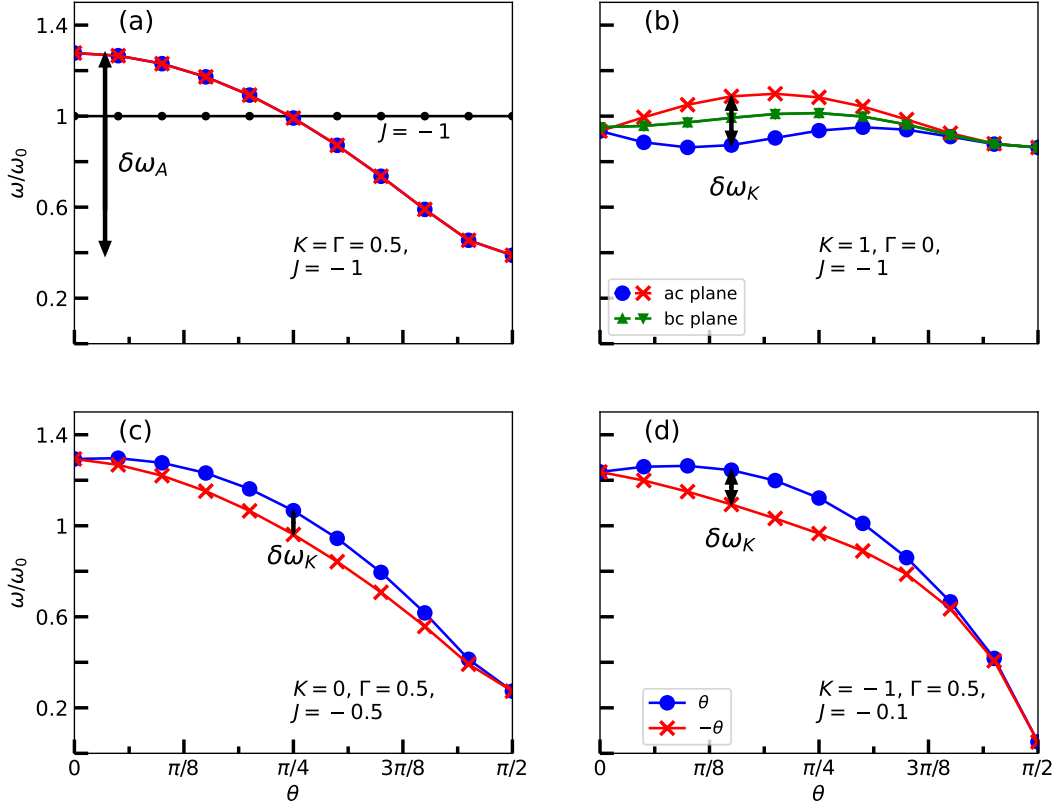


FIG. 2. Angle-dependent spin excitations in FMR for spin  $\frac{1}{2}$  using ED on a  $C_3$ -symmetric 24-site cluster with Zeeman energy  $g\mu_B h = 1$  and various sets of parameters. The standard anisotropy  $\delta\omega_A$  and the anisotropy between magnetic field angles of  $\theta$  (blue) and  $-\theta$  (red),  $\delta\omega_K$  are highlighted. (a)  $J = -1$  and  $K = \Gamma = 0.5$ . (b)  $J = -1$ ,  $K = 1$ , and  $\Gamma = 0$ . FMR in the  $b - c$  plane is shown in green:  $\theta$  (up triangle) and  $-\theta$  (down triangle). (c)  $J = -0.5$ ,  $\Gamma = 0.5$ , and  $K = 0$ . (d)  $J = -0.1$ ,  $K = -1$ ,  $\Gamma = 0.5$ . See the main text for implication of the results.

We set our units the magnetic field  $h = 1$  and  $g = \mu_B \equiv 1$ , leading to the excitation energy of a free spin,  $\omega_0 = g\mu_B h = 1$ , so the excitation energies calculated are normalized by  $\omega_0$ . A few sets of different interaction parameters (in units of  $\omega_0$ ) are investigated. In Fig. 2, the panel (a) shows the  $J = -1$  and  $K = \Gamma = 0.5$  case with no  $\delta\omega_K(\theta)$  between  $-\pi/2 < \theta < 0$  (red line) and  $0 < \theta < \pi/2$  (blue line), since  $J_{ac} = 0$ . The conventional anisotropy  $\delta\omega_A$  is finite, because the  $\Gamma$  interaction generates a strong anisotropy between



the plane  $\theta = 0$  and the c-axis  $\theta = \pi/2$ , i.e.,  $J_X \neq J_Z$  due to a finite  $\Gamma$  contribution. The black line is for only  $J = -1$  showing a uniform FMR independent of angles which serves as a reference. The panel (b) shows the  $J = -1$ ,  $K = 1$ , and  $\Gamma = 0$  case, which shows a finite  $\delta\omega_K(\theta)$  between  $-\pi/2 < \theta < 0$  and  $0 < \theta < \pi/2$  in the  $a - c$  plane. On the other hand, no  $\delta\omega_K(\theta)$  by sweeping  $\theta$  in the  $b - c$  plane (up and down triangles with green line) is observed, consistent with the symmetry analysis presented above. Note the conventional anisotropy  $\delta\omega_A$  in both  $a - c$  and  $b - c$  planes are not exactly zero, because the Kitaev interaction selects the magnetic moment along the cubic axes in the ferromagnetic state via order by disorder<sup>31,40</sup>. This leads to a tiny anisotropy between the plane  $\theta = 0$  and the c-axis  $\theta = \pi/2$  when  $\Gamma = 0$  and  $J_X = J_Z$ . This anisotropy becomes weaker when the magnetic field increases, i.e, when the moment polarization overcomes the order by disorder effect. The Supplementary Figure S1 shows that the anisotropy is almost gone when the field is increased by three times with the same set of parameters, where the Heisenberg limit (black line) is added for a reference. When  $\Gamma$  becomes finite, this conventional anisotropy is determined by the  $\Gamma$  interaction as shown in the other panels, and the order by disorder effect becomes silent. Comparison to the finite  $\Gamma$  cases with increased field strength is also presented in the Supplementary. The panel (c) shows the  $J = -0.5$ ,  $\Gamma = 0.5$ , and  $K = 0$  case. The  $\Gamma$  interaction alone can generate a finite  $\delta\omega_K$  due to the broken  $C_{2a}$  by  $J_{ac}$ . In addition, the  $\Gamma$  interaction generates a large  $\delta\omega_A$ , different from the panel (b). The panel (d) presents the  $J = -0.1$ ,  $K = -1$  and  $\Gamma = 0.5$  case, which is close to a set of parameters proposed for  $J_{\text{eff}} = \frac{1}{2}$  Kitaev candidate materials<sup>28</sup>. Clearly,  $\delta\omega_K(\theta)$  is significant due to a finite  $J_{ac}$ , and  $\delta\omega_A$  is also large due to a finite  $\Gamma$ . While a magnetic field of strength  $h = 1$  is used to polarize the ground state where the finite-size effect is small as shown in the Supplementary Figure 2, our symmetry argument works for any finite field. However, we note that the finite-size effect of ED is minimal when the ground state is polarized.

**Inelastic Neutron Scattering** – Complementary to FMR, INS can measure excitations between different points in the reciprocal space based on the momentum transfer of the scattered neutrons. The magnon dispersions of the ordered states of magnetic materials measured via INS have been used to determine the spin exchange Hamiltonian parameters<sup>10,17,41–45</sup>. Figure 3(a) and (b) show the spin excitations at accessible wavevectors on a  $C_3$ -symmetric 24-site cluster with the same parameters for Fig. 2(d) for  $h = 1$  and  $h = 8$ , respectively. The cluster and the accessible momenta are shown in (c) and (d),

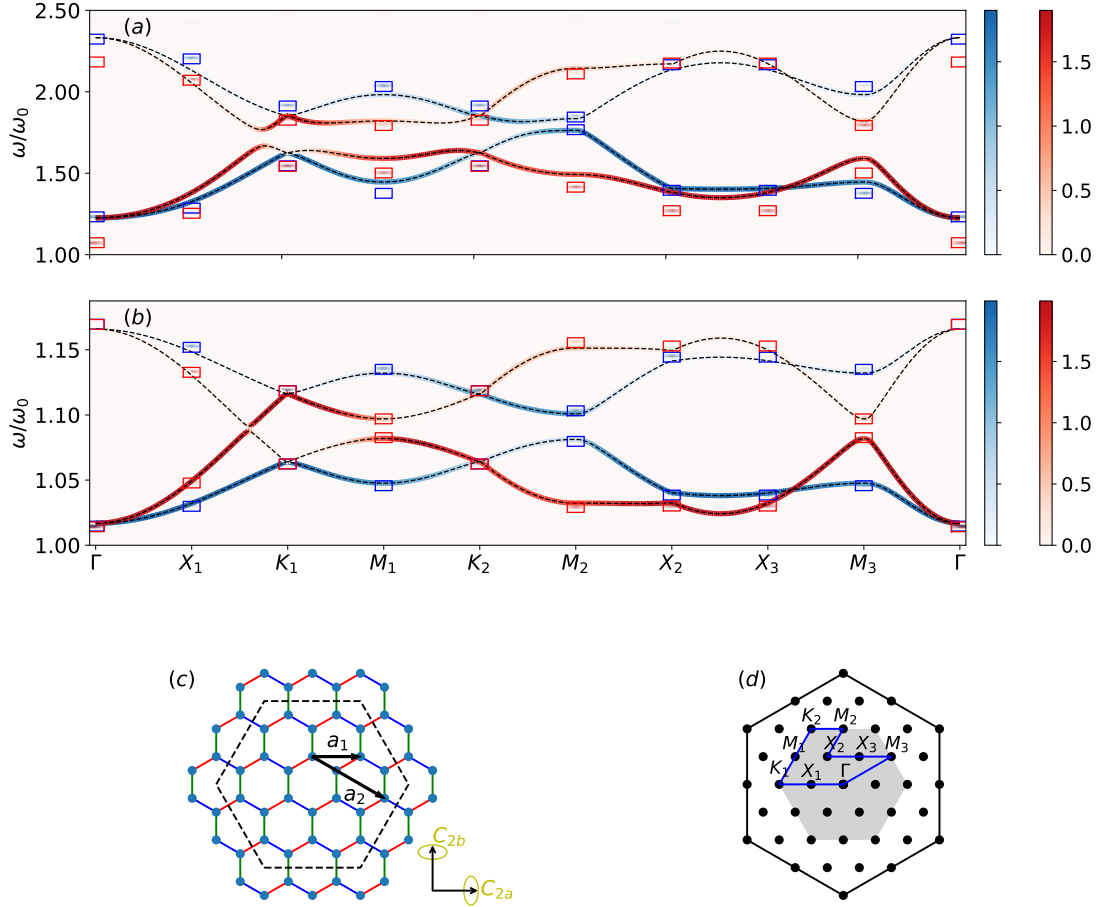


FIG. 3. Dynamic spin structure factor (DSSF) of the spin excitations at accessible wavevectors for spin  $\frac{1}{2}$  using ED on a  $C_3$ -symmetric 24-site cluster are shown by red and blue boxes, with the same parameters for Fig. 2(d), i.e.  $(J, K, \Gamma) = (-0.1, -1, 0.5)$ , equivalent to  $(J_X, J_Z, J_{ab}, J_{ac}) = (-0.6, -0.1, 0, -0.5)$  in units of  $\omega_0$ . The magnetic field angles in the  $a-c$  plane are  $30^\circ$  (blue) and  $-30^\circ$  (red). The dashed lines are DSSF obtained by LSWT. (b) DSSF with the same parameter set as (a) except the field  $h = 8$  shows a better match between the ED and LSWT results; see the main text for further discussions. The colour bars represent the intensity of DSSF. (c)  $C_3$ -symmetric 24-site cluster used for the ED. (d) Accessible momentum points labeled in x-axis of (a) and (b).

respectively. We set the magnetic field angles  $\theta = 30^\circ$  (blue) and  $\theta = -30^\circ$  (red) in the  $a-c$  plane. The square boxes denote the excitation energies, and the colour bars indicate the intensity of DSSF  $\sum_{\alpha} S^{\alpha\alpha}(\mathbf{q}, \omega)$  (details can be found in the Methods). The structure factor is convolved with a Gaussian of finite width to emulate finite experimental resolution. We observe a clear difference between the two field directions,  $\delta\omega_K$  at every momentum points.

In particular,  $\delta\omega_K$  is the largest at  $M_2$ -point, while it is tiny at the  $K$ -points. Since the  $C_{2b}$  and inversion symmetries are intact,  $M_1$  and  $M_3$  share the same energies.

To gain more insights of  $\delta\omega_K(\theta)$  at finite momenta obtained by ED, we also perform LSWT calculations with the magnetization making an angle  $\theta_M$  as indicated in Fig. 1(b).  $\theta_M$  is found via minimizing the classical ground state energy (details can be found in the Methods); the LSWT with the set of parameters used for Fig. 3(a)'s ED result leads to  $\theta_M \sim 12.1^\circ$ . The spin excitations within the LSWT are shown as dashed lines together with the ED results in Fig. 3(a). The mismatch between LSWT and ED is visible at every momenta, which implies the significant effects of nonlinear terms<sup>46</sup>.

However, when the field increases, the difference should decrease, since a more polarized state is achieved at a higher field. In Fig. 3(b), we show both ED and LSWT with  $h = 8$  and  $\theta_M \sim 25.8^\circ$ , where the two results match well as expected, and the nonlinear terms become less significant. In particular, the anisotropy  $\delta\omega_K$  at the  $K$ -point at the high field limit given by the leading terms in  $1/h$ , is simplified as

$$\begin{aligned} \delta\omega_K(\theta) = & \frac{3}{8} \cos \theta_M \left( |2\sqrt{2}J_{ac} \sin \theta_M - J_{ab} \cos \theta_M| - |2\sqrt{2}J_{ac} \sin \theta_M + J_{ab} \cos \theta_M| \right) \\ & + \frac{9\sqrt{2}J_{ac}J_{ab} (2 \sin 2\theta_M + \sin 4\theta_M)}{128h \cos(\theta - \theta_M)} + \mathcal{O}\left(\frac{1}{h^2}\right), \end{aligned} \quad (10)$$

where  $\theta_M(\theta) \rightarrow \theta$  when  $h$  is the largest energy scale. This shows that both  $J_{ac}$  and  $J_{ab}$  should be finite for a finite  $\delta\omega_K$  at the  $K$ -point, which explains no splitting of  $\delta\omega_K$  at the  $K$ -point in Fig. 3(b), as our choice of parameters gives  $J_{ab} = 0$ , i.e,  $\Gamma = -K/2$ . On the other hand, at the  $M_2$ -point, there is no simple expression, but the leading terms of  $\delta\omega_K(\theta)$  in  $\delta\theta_{a/c}$  around the  $a$ - and  $c$ -axis ( $\delta\theta_a = 0 - \theta$  and  $\delta\theta_c = \theta - \pi/2$ ) are given by

$$\delta\omega_K(\theta) \simeq \begin{cases} J_{ac}(\delta\theta_a)A + \mathcal{O}(\delta\theta_a^3) \\ J_{ac}(\delta\theta_c)C + \mathcal{O}(\delta\theta_c^3), \end{cases} \quad (11)$$

where  $A$  and  $C$  are functions of other interactions given in the Supplementary Section 2. Clearly,  $\delta\omega_K(\theta)$  appears as odd powers of  $J_{ac}$  and  $\delta\theta_{a/c}$ , consistent with the symmetry analysis presented above.

So far, we have focused on the ideal octahedra environment. However, trigonal distortion is often present, albeit small, which introduces extra exchange interactions. Below we discuss other contributions to  $\delta\omega_A$  complicating the isolation of  $K$  from  $J_{ac}$  and our resolution of such complication in order to estimate the Kitaev interaction out of a full Hamiltonian.

**Effects of trigonal distortion and further neighbour interactions** – In principle, there are other small but finite interactions; few examples in  $\delta\mathcal{H}'$  include

$$\begin{aligned} \delta\mathcal{H}' = & \sum_{\langle ij \rangle \in \alpha\beta(\gamma)} \left[ \Gamma' (S_i^\alpha S_j^\gamma + S_i^\gamma S_j^\alpha + S_i^\beta S_j^\gamma + S_i^\gamma S_j^\beta) \right] \\ & + J_2 \sum_{\langle\langle i,j \rangle\rangle} \mathbf{S}_i \cdot \mathbf{S}_j + J_3 \sum_{\langle\langle\langle i,j \rangle\rangle\rangle} \mathbf{S}_i \cdot \mathbf{S}_j, \end{aligned} \quad (12)$$

where  $\Gamma'$  is introduced when a trigonal distortion is present<sup>26</sup>;  $J_2$  and  $J_3$  are the second and third n.n. Heisenberg interactions respectively. It is natural to expect that they are smaller than the n.n. Kitaev, Gamma, and Heisenberg interactions<sup>18,27,28</sup>. Several types of interlayer exchange interactions are present, but they are even smaller than the terms considered in Eq. 12<sup>18</sup>.

Let's investigate how they affect the above analysis done for the ideal n.n. Hamiltonian. First of all, the isotropic interactions such as further neighbour  $J_2$ ,  $J_3$ , and the interlayer Heisenberg do not make any change to our proposal, since they do not contribute to  $\delta\omega_A$  nor  $\delta\omega_K$ . On the other hand, the  $\Gamma'$  modifies the exchange parameters as follows:

$$\begin{aligned} J_X &= J + J_{ac} - \Gamma', \quad J_Z = J + J_{ab} + 2\Gamma', \\ J_{ab} &= \frac{1}{3}K + \frac{2}{3}(\Gamma - \Gamma'), \quad J_{ac} = \frac{1}{3}K - \frac{1}{3}(\Gamma - \Gamma'). \end{aligned} \quad (13)$$

The conventional anisotropy  $\delta\omega_A$  is now due to  $\Gamma + 2\Gamma'$  obtained from  $J_Z - J_X$ . Thus to single out the Kitaev interaction, one has to find both  $\Gamma$  and  $\Gamma'$ , as  $J_{ac}$  is a combination of  $K$ ,  $\Gamma$  and  $\Gamma'$ . Once the trigonal distortion is present, the g-factor also becomes anisotropic, i.e., the in-plane  $g_a$  is different from the c-axis  $g_c$ , which affects  $\delta\omega_A$ .

However, the g-factor anisotropy does not affect the  $\delta\omega_K$ , since the field angles of  $\theta$  and  $-\theta$  involve the same strength of in- and out-of-plane field components, i.e,  $\mathbf{h}(\theta) = h_a\hat{a} + h_c\hat{c}$  and  $\mathbf{h}(-\theta) = -h_a\hat{a} + h_c\hat{c}$ . Thus we wish to extract the information of  $K$  and  $\Gamma - \Gamma'$  from  $\delta\omega_K$ , as it is free from the g-factor anisotropy.

We note that  $\delta\omega_K$  at the K-point, Eq. (10) offers both  $J_{ac}$  and  $J_{ab}$  from the first term independent of the field and the next term proportional to  $1/h_{\text{eff}}$  ( $h_{\text{eff}} = h\sqrt{g_a^2 \cos^2 \theta + g_c^2 \sin^2 \theta}$ ). Once  $J_{ac}$  and  $J_{ab}$  are deduced,  $K$  and  $\Gamma - \Gamma'$  can be estimated from Eq. (13). The measurements of  $\delta\omega_K$  at the K-point with a large magnetic field then determine  $K$  and  $\Gamma - \Gamma'$  separately. Further neighbor Heisenberg interactions,  $J_2$  and  $J_3$  do not modify Eq. (10) in the high-field limit, so they do not affect our procedure.

## DISCUSSION

We propose an experimental setup to single out the Kitaev interaction for honeycomb Mott insulators with edge-sharing octahedra. In an ideal octahedra cage, the symmetry-allowed n.n. interactions contain the Kitaev, another bond-dependent  $\Gamma$  and Heisenberg interactions. We prove that the magnetic anisotropy related by the  $\pi$ -rotation around the  $a$ -axis denoted by  $\delta\omega_K$  occurs only when a combination of  $K$  and  $\Gamma$ , i.e.  $K - \Gamma$ , is finite. This can be measured from the spin excitation energy differences under the magnetic field of angle sweeping from above to below the honeycomb plane using the FMR or INS techniques. Since the in- and out-of-plane magnetic anisotropy,  $\delta\omega_A$  is determined solely by  $\Gamma$ , one can estimate  $\Gamma$  strength first from  $\delta\omega_A$  and then extract the Kitaev interaction from  $\delta\omega_K$ .

While the trigonal distortion introduces an additional interaction, the Kitaev interaction is unique as it is the only interaction that contributes to  $\delta\omega_K$  without altering  $\delta\omega_A$ . Our theory is applicable to all Kitaev candidate materials including an emerging candidate  $\text{RuCl}_3$ . In particular, since the two dominant interactions are ferromagnetic Kitaev and positive  $\Gamma$  interactions in  $\text{RuCl}_3$ <sup>3,5,18,27</sup>, leading to a large  $J_{ac}$  and a small  $J_{ab}$ , we predict that  $\delta\omega_K$  independent of the g-factor anisotropy is significant except at the  $K$ -point. The Supplementary Figure 3 shows the FMR and INS of a set of parameters with a small negative  $\Gamma'$  interaction to stabilize a zero-field zig-zag ground state as in  $\text{RuCl}_3$ <sup>18,27,28</sup>. Another relevant perturbation in some materials is the effect of monoclinic structure which loses the  $C_{3c}$  symmetry of  $R\bar{3}$ , making the z-bond different from the x- and y-bond. The current theory of finite  $\delta\omega_K$  due to a finite  $J_{ac}$  still works for  $C2/m$  structure. However, since the z-bond of  $J_{ac}^z = K_z/3 - \Gamma_z/3$  is no longer the same as the x- and y-bond of  $J_{ac}^x = J_{ac}^y$  and  $C_{2a}$  symmetry relates between the x- and y-bond, the anisotropy  $\delta\omega_K$  only detects  $J_{ac}^x = K_x/3 - \Gamma_x/3$  where  $K_x = K_y$  and  $\Gamma_x = \Gamma_y$ .

The symmetry-based theory presented here is also valid for higher spin models with the Kitaev interaction such as  $S = 3/2$   $\text{CrI}_3$  including a nonzero single-ion anisotropy<sup>19,21,22,47</sup> which generates a further anisotropy in  $\delta\omega_A$  but does not affect the  $\delta\omega_K$ . The next nearest neighbor Dzyaloshinskii-Moriya interaction with the d-vector along the c-axis<sup>48</sup> is also invariant under the  $C_{2a}$  symmetry. Further studies for higher-spin models remain to be investigated to identify higher-spin Kitaev spin liquid. We would like to emphasize that the proposed set-up is suitable for other experimental techniques such as low-energy tera-

hertz optical and nuclear magnetic resonance spectroscopies that probe spin excitations in addition to the angle-dependent FMR and INS spectroscopy shown in this work as examples.

## METHODS

**Exact Diagonalization Simulations** – Numerical ED was used to compute spin excitations under a magnetic field. ED was performed on a 24-site honeycomb cluster with periodic boundary conditions, where the Lanczos method<sup>49,50</sup> was used to obtain the lowest-lying eigenvalues and eigenvectors of the Hamiltonian in Eq. (2). The 24-site honeycomb shape and accessible momentum points in the Brillouin zone are shown in the Supplementary Figure 1. The probability of the spin excitation of momentum  $\mathbf{q}$  and energy  $\omega$  is proportional to the dynamic spin structure factor<sup>51</sup> (DSSF) given by

$$\begin{aligned}
S^{\alpha\beta}(\mathbf{q}, \omega) &= \frac{1}{N} \sum_{i,j} e^{-i\mathbf{q}\cdot(\mathbf{R}_i - \mathbf{R}_j)} \int_{-\infty}^{\infty} dt e^{i\omega t} \langle S_i^\alpha(t) S_j^\beta(0) \rangle \\
&= \frac{1}{N} \sum_{i,j} e^{-i\mathbf{q}\cdot(\mathbf{R}_i - \mathbf{R}_j)} \sum_{\lambda,\lambda'} p_\lambda \langle \lambda | S_i^\alpha | \lambda' \rangle \langle \lambda' | S_j^\beta | \lambda \rangle \delta(\hbar\omega + E_\lambda - E_{\lambda'}) \\
&= \sum_{\lambda,\lambda'} p_\lambda \langle \lambda | S_{-\mathbf{q}}^\alpha | \lambda' \rangle \langle \lambda' | S_{\mathbf{q}}^\beta | \lambda \rangle \delta(\hbar\omega + E_\lambda - E_{\lambda'}),
\end{aligned} \tag{14}$$

where the Lehmann representation is used;  $|\lambda\rangle$  and  $|\lambda'\rangle$  are the eigenstates with the thermal population factor  $p_\lambda$ , and  $S^{\alpha,\beta}$  are the spin operators. In the low temperatures, we take  $|\lambda\rangle$  to be the ground state  $|0\rangle$  and we are interested in the lowest energy excitation to  $|1\rangle$  with a nonzero probability. For optical spectroscopies such as FMR,  $\alpha = \beta =$  direction of the RF electromagnetic field and  $\mathbf{q} = 0$ , so  $|0\rangle$  and  $|1\rangle$  belong to the same momentum sector. The structure factor simplifies to

$$S^{\alpha\alpha}(\omega) = \frac{1}{N} \left| \langle 1 | \sum_i S_i^\alpha | 0 \rangle \right|^2 \delta(\hbar\omega + E_0 - E_1).$$

For INS, the finite  $\mathbf{q}$  must match the difference in the momenta of  $|0\rangle$  and  $|1\rangle$ . For simplicity, we calculate the DSSF for  $\alpha = \beta$ ,

$$\sum_{\alpha} S^{\alpha\alpha}(\mathbf{q}, \omega) = \sum_{\alpha} |\langle 1 | S_{\mathbf{q}}^\alpha | 0 \rangle|^2 \delta(\hbar\omega + E_0 - E_1).$$

**Linear Spin Wave Theory** – The Hamiltonian in Eq. (2) is bosonized by the standard

Holstein-Primakoff transformation<sup>52</sup> expanded to linear order in the spin  $S$ :

$$\begin{aligned}
S_j^+ &= S_j^a + iS_j^b = \sqrt{2S} \left( a_j - \frac{a_j^\dagger a_j a_j}{4S} + \mathcal{O}\left(\frac{1}{S^2}\right) \right) \simeq \sqrt{2S} a_j \\
S_j^- &= S_j^a - iS_j^b = \sqrt{2S} \left( a_j^\dagger - \frac{a_j^\dagger a_j^\dagger a_j}{4S} + \mathcal{O}\left(\frac{1}{S^2}\right) \right) \simeq \sqrt{2S} a_j^\dagger \\
S_j^c &= S^c - a_j^\dagger a_j,
\end{aligned} \tag{15}$$

where the quantization axis is parallel to the c-axis. The Fourier transforms are  $a_j = \frac{1}{\sqrt{N}} \sum_{\mathbf{k}} e^{i\mathbf{k}\cdot\mathbf{r}_j} a_{\mathbf{k}}$  for sublattice A and  $b_j = \frac{1}{\sqrt{N}} \sum_{\mathbf{k}} e^{i\mathbf{k}\cdot(\mathbf{r}_j+\delta)} b_{\mathbf{k}}$  for sublattice B, where  $\delta$  is the vector pointing to nearest neighbors. The resulting quadratic Hamiltonian has the form  $\mathcal{H} = \sum_{\mathbf{k}} X^\dagger H(\mathbf{k}) X$ , where  $X^\dagger = (a_{\mathbf{k}}^\dagger, b_{\mathbf{k}}^\dagger, a_{-\mathbf{k}}, b_{-\mathbf{k}})$ . Diagonalizing this BdG Hamiltonian following standard methods<sup>53</sup> gives two spin wave excitation branches.

For a general field, the Hamiltonian in Eq. (2) is first written in new axes  $\mathbf{a}'\mathbf{b}'\mathbf{c}'$ .  $\hat{a}' = (\sin \theta \cos \phi, \sin \theta \sin \phi, -\cos \theta)$ ,  $\hat{b}' = (-\sin \phi, \cos \phi, 0)$ , and  $\hat{c}' = (\cos \theta \cos \phi, \cos \theta \sin \phi, \sin \theta)$ .  $\hat{c}'$  is parallel to the magnetization  $\theta_M$ , which is not the same direction as the magnetic field, unless the field is very large to fully polarize the moment. The magnetization angle  $\theta_M$  is obtained by minimizing the classical ground state energy; the azimuthal angle of the magnetization is the same as that of the field  $\phi$ . Then, LSWT is applied on the ground state.<sup>46</sup> Arbitrary  $\hat{a}'$  and  $\hat{b}'$  axes obtained by rotation around  $\hat{c}'$  are valid and do not affect the result.

---

\* [hykee@physics.utoronto.ca](mailto:hykee@physics.utoronto.ca)

<sup>1</sup> William Witczak-Krempa, Gang Chen, Yong Baek Kim, and Leon Balents, “Correlated quantum phenomena in the strong spin-orbit regime,” [Annual Review of Condensed Matter Physics](#) **5**, 57–82 (2014).

<sup>2</sup> Jeffrey G. Rau, Eric Kin-Ho Lee, and Hae-Young Kee, “Spin-orbit physics giving rise to novel phases in correlated systems: Iridates and related materials,” [Annual Review of Condensed Matter Physics](#) **7**, 195–221 (2016).

<sup>3</sup> Stephen M. Winter, Alexander A. Tsirlin, Maria Daghofer, Jeroen van den Brink, Yogesh Singh, Philipp Gegenwart, and Roser Valentí, “Models and materials for generalized Kitaev magnetism,” [Journal of Physics: Condensed Matter](#) **29**, 493002 (2017).

- <sup>4</sup> M. Hermanns, I. Kimchi, and J. Knolle, “Physics of the Kitaev model: Fractionalization, dynamic correlations, and material connections,” *Annual Review of Condensed Matter Physics* **9**, 17–33 (2018).
- <sup>5</sup> Lukas Janssen and Matthias Vojta, “Heisenberg-kitaev physics in magnetic fields,” *Journal of Physics: Condensed Matter* **31**, 423002 (2019).
- <sup>6</sup> Tomohiro Takayama, Jiří Chaloupka, Andrew Smerald, Giniyat Khaliullin, and Hidenori Takagi, “Spin–orbit-entangled electronic phases in 4d and 5d transition-metal compounds,” *Journal of the Physical Society of Japan* **90**, 062001 (2021), <https://doi.org/10.7566/JPSJ.90.062001>.
- <sup>7</sup> Alexei Kitaev, “Anyons in an exactly solved model and beyond,” *Ann. Phys. (N. Y.)* **321**, 2 – 111 (2006), January Special Issue.
- <sup>8</sup> George Jackeli and Giniyat Khaliullin, “Mott insulators in the strong spin-orbit coupling limit: From Heisenberg to a quantum compass and Kitaev models,” *Phys. Rev. Lett.* **102**, 017205 (2009).
- <sup>9</sup> Yogesh Singh, S. Manni, J. Reuther, T. Berlijn, R. Thomale, W. Ku, S. Trebst, and P. Gegenwart, “Relevance of the Heisenberg-Kitaev model for the honeycomb lattice iridates  $A_2IrO_3$ ,” *Phys. Rev. Lett.* **108**, 127203 (2012).
- <sup>10</sup> S. K. Choi, R. Coldea, A. N. Kolmogorov, T. Lancaster, I. I. Mazin, S. J. Blundell, P. G. Radaelli, Yogesh Singh, P. Gegenwart, K. R. Choi, S.-W. Cheong, P. J. Baker, C. Stock, and J. Taylor, “Spin waves and revised crystal structure of honeycomb iridate  $Na_2IrO_3$ ,” *Phys. Rev. Lett.* **108**, 127204 (2012).
- <sup>11</sup> K. W. Plumb, J. P. Clancy, L. J. Sandilands, V. Vijay Shankar, Y. F. Hu, K. S. Burch, Hae-Young Kee, and Young-June Kim, “ $\alpha$ - $RuCl_3$ : A spin-orbit assisted mott insulator on a honeycomb lattice,” *Phys. Rev. B* **90**, 041112(R) (2014).
- <sup>12</sup> K. A. Modic, Tess E. Smidt, Itamar Kimchi, Nicholas P. Breznay, Alun Biffin, Sungkyun Choi, Roger D. Johnson, Radu Coldea, Pilanda Watkins-Curry, Gregory T. McCandless, Julia Y. Chan, Felipe Gandara, Z. Islam, Ashvin Vishwanath, Arkady Shekhter, Ross D. McDonald, and James G. Analytis, “Realization of a three-dimensional spin-anisotropic harmonic honeycomb iridate,” *Nat. Commun.* **5**, 4203 (2014).
- <sup>13</sup> Heung-Sik Kim, Vijay Shankar V., Andrei Catuneanu, and Hae-Young Kee, “Kitaev magnetism in honeycomb  $\alpha$ - $RuCl_3$  with intermediate spin-orbit coupling,” *Phys. Rev. B* **91**, 241110(R) (2015).



- <sup>14</sup> J. A. Sears, M. Songvilay, K. W. Plumb, J. P. Clancy, Y. Qiu, Y. Zhao, D. Parshall, and Young-June Kim, “Magnetic order in  $\alpha$ -RuCl<sub>3</sub>: A honeycomb-lattice quantum magnet with strong spin-orbit coupling,” *Phys. Rev. B* **91**, 144420 (2015).
- <sup>15</sup> Luke J. Sandilands, Yao Tian, Kemp W. Plumb, Young-June Kim, and Kenneth S. Burch, “Scattering continuum and possible fractionalized excitations in  $\alpha$ -RuCl<sub>3</sub>,” *Phys. Rev. Lett.* **114**, 147201 (2015).
- <sup>16</sup> R. D. Johnson, S. C. Williams, A. A. Haghighirad, J. Singleton, V. Zapf, P. Manuel, I. I. Mazin, Y. Li, H. O. Jeschke, R. Valentí, and R. Coldea, “Monoclinic crystal structure of  $\alpha$ -RuCl<sub>3</sub> and the zigzag antiferromagnetic ground state,” *Phys. Rev. B* **92**, 235119 (2015).
- <sup>17</sup> A. Banerjee, C. A. Bridges, J.-Q. Yan, A. A. Aczel, L. Li, M. B. Stone, G. E. Granroth, M. D. Lumsden, Y. Yiu, J. Knolle, S. Bhattacharjee, D. L. Kovrizhin, R. Moessner, D. A. Tennant, D. G. Mandrus, and S. E. Nagler, “Proximate Kitaev quantum spin liquid behaviour in a honeycomb magnet,” *Nature Materials* **15**, 733 (2016), article.
- <sup>18</sup> Heung-Sik Kim and Hae-Young Kee, “Crystal structure and magnetism in  $\alpha$ -RuCl<sub>3</sub>: An ab initio study,” *Phys. Rev. B* **93**, 155143 (2016).
- <sup>19</sup> P. Peter Stavropoulos, D. Pereira, and Hae-Young Kee, “Microscopic mechanism for a higher-spin kitaev model,” *Phys. Rev. Lett.* **123**, 037203 (2019).
- <sup>20</sup> J L Lado and J Fernández-Rossier, “On the origin of magnetic anisotropy in two dimensional CrI<sub>3</sub>,” *2D Mater.* **4**, 035002 (2017).
- <sup>21</sup> Changsong Xu, Junsheng Feng, Hongjun Xiang, and Laurent Bellaiche, “Interplay between kitaev interaction and single ion anisotropy in ferromagnetic cri<sub>3</sub> and crgete<sub>3</sub> monolayers,” *npj Computational Materials* **4**, 57 (2018).
- <sup>22</sup> Inhee Lee, Franz G. Utermohlen, Daniel Weber, Kyusung Hwang, Chi Zhang, Johan van Tol, Joshua E. Goldberger, Nandini Trivedi, and P. Chris Hammel, “Fundamental spin interactions underlying the magnetic anisotropy in the kitaev ferromagnet cri<sub>3</sub>,” *Phys. Rev. Lett.* **124**, 017201 (2020).
- <sup>23</sup> Jiří Chaloupka, George Jackeli, and Giniyat Khaliullin, “Kitaev-Heisenberg model on a honeycomb lattice: Possible exotic phases in iridium oxides A<sub>2</sub>IrO<sub>3</sub>,” *Phys. Rev. Lett.* **105**, 027204 (2010).
- <sup>24</sup> Jiří Chaloupka, George Jackeli, and Giniyat Khaliullin, “Zigzag magnetic order in the iridium oxide Na<sub>2</sub>IrO<sub>3</sub>,” *Phys. Rev. Lett.* **110**, 097204 (2013).

- <sup>25</sup> Jeffrey G. Rau, Eric Kin-Ho Lee, and Hae-Young Kee, “Generic spin model for the honeycomb iridates beyond the Kitaev limit,” *Phys. Rev. Lett.* **112**, 077204 (2014).
- <sup>26</sup> Jeffrey G. Rau and Hae-Young Kee, “Trigonal distortion in the honeycomb iridates: Proximity of zigzag and spiral phases in  $\text{Na}_2\text{IrO}_3$ ,” [arXiv:1408.4811 \[cond-mat.str-el\]](#).
- <sup>27</sup> Stephen M. Winter, Ying Li, Harald O. Jeschke, and Roser Valentí, “Challenges in design of Kitaev materials: Magnetic interactions from competing energy scales,” *Phys. Rev. B* **93**, 214431 (2016).
- <sup>28</sup> Lukas Janssen, Eric C. Andrade, and Matthias Vojta, “Magnetization processes of zigzag states on the honeycomb lattice: Identifying spin models for  $\alpha\text{-RuCl}_3$  and  $\text{Na}_2\text{IrO}_3$ ,” *Phys. Rev. B* **96**, 064430 (2017).
- <sup>29</sup> Qiang Luo, Jize Zhao, Hae-Young Kee, and Xiaoqun Wang, “Gapless quantum spin liquid in a honeycomb  $\gamma$  magnet,” *npj Quantum Materials* **6**, 57 (2021).
- <sup>30</sup> P. A. Maksimov and A. L. Chernyshev, “Rethinking  $\alpha\text{-rucl}_3$ ,” *Phys. Rev. Research* **2**, 033011 (2020).
- <sup>31</sup> Jiří Chaloupka and Giniyat Khaliullin, “Magnetic anisotropy in the kitaev model systems  $\text{na}_2\text{iro}_3$  and  $\text{rucl}_3$ ,” *Phys. Rev. B* **94**, 064435 (2016).
- <sup>32</sup> Kate A. Ross, Lucile Savary, Bruce D. Gaulin, and Leon Balents, “Quantum Excitations in Quantum Spin Ice,” *Physical Review X* **1**, 1–10 (2011), [arXiv:1107.0761](#).
- <sup>33</sup> Jiří Chaloupka and Giniyat Khaliullin, “Hidden symmetries of the extended kitaev-heisenberg model: Implications for the honeycomb-lattice iridates  $A_2\text{iro}_3$ ,” *Phys. Rev. B* **92**, 024413 (2015).
- <sup>34</sup> Zhang Z, Zhou L, Wigen PE, and Ounadjela K, “Angular dependence of ferromagnetic resonance in exchange-coupled Co/Ru/Co trilayer structures,” *Physical review. B, Condensed matter* **50**, 6094–6112 (1994).
- <sup>35</sup> Heinrich B, Tserkovnyak Y, Woltersdorf G, Brataas A, Urban R, and Bauer GE, “Dynamic exchange coupling in magnetic bilayers,” *Physical review letters* **90**, 4 (2003).
- <sup>36</sup> V. P. Nascimento, E. Baggio Saitovitch, F. Pelegrini, L. C. Figueiredo, A. Biondo, and E. C. Passamani, “Ferromagnetic resonance study of the exchange bias field in NiFe,FeMn,NiFe trilayers,” *Journal of Applied Physics* **99**, 08C108 (2006).
- <sup>37</sup> K Lenz, E Kosubek, T Toliński, J Lindner, and K Baberschke, “In situ ferromagnetic resonance in coupled ultrathin trilayers with perpendicularly oriented easy axes,” *Journal of Physics: Condensed Matter* **15**, 7175 (2003).

- <sup>38</sup> M. Díaz de Sihues, C. A. Durante-Rincón, and J. R. Fermin, “A ferromagnetic resonance study of NiFe alloy thin films,” [Journal of Magnetism and Magnetic Materials](#) **316** (2007), [10.1016/J.JMMM.2007.02.181](#).
- <sup>39</sup> Gavriljuk VG, Dobrinsky A, Shanina BD, and Kolesnik SP, “A study of the magnetic resonance in a single-crystal Ni(50.47)Mn(28.17)Ga(21.36) alloy,” [Journal of physics. Condensed matter : an Institute of Physics journal](#) **18**, 7613–7627 (2006).
- <sup>40</sup> P. Peter Stavropoulos, Andrei Catuneanu, and Hae-Young Kee, “Counter-rotating spiral order in three-dimensional iridates: Signature of hidden symmetry in the kitaev- $\Gamma$  model,” [Phys. Rev. B](#) **98**, 104401 (2018).
- <sup>41</sup> G. Shirane, V. J. Minkiewicz, and R. Nathans, “Spin Waves in 3d Metals,” [Journal of Applied Physics](#) **39**, 383 (1968).
- <sup>42</sup> Y. Endoh, G. Shirane, R. J. Birgeneau, Peter M. Richards, and S. L. Holt, “Dynamics of an  $s$ - $d$  spin class,” [Physical Review Letters](#) **32**, 170 (1974).
- <sup>43</sup> Kejing Ran, Jinghui Wang, Wei Wang, Zhao Yang Dong, Xiao Ren, Song Bao, Shichao Li, Zhen Ma, Yuan Gan, Youtian Zhang, J. T. Park, Guochu Deng, S. Danilkin, Shun Li Yu, Jian Xin Li, and Jinsheng Wen, “Spin-Wave Excitations Evidencing the Kitaev Interaction in Single Crystalline  $\alpha$ -RuCl<sub>3</sub>,” [Physical Review Letters](#) **118**, 107203 (2017), [arXiv:1702.04920](#).
- <sup>44</sup> Seung Hwan Do, Sang Youn Park, Junki Yoshitake, Joji Nasu, Yukitoshi Motome, Yong Seung Kwon, D. T. Adroja, D. J. Voneshen, Kyoo Kim, T. H. Jang, J. H. Park, Kwang Yong Choi, and Sungdae Ji, “Majorana fermions in the Kitaev quantum spin system  $\alpha$ -RuCl<sub>3</sub>,” [Nature Physics](#) **2017 13:11** **13**, 1079–1084 (2017).
- <sup>45</sup> Arnab Banerjee, Paula Lampen-Kelley, Johannes Knolle, Christian Balz, Adam Anthony Aczel, Barry Winn, Yaohua Liu, Daniel Pajerowski, Jiaqiang Yan, Craig A. Bridges, Andrei T. Savici, Bryan C. Chakoumakos, Mark D. Lumsden, David Alan Tennant, Roderich Moessner, David G. Mandrus, and Stephen E. Nagler, “Excitations in the field-induced quantum spin liquid state of  $\alpha$ -rucl<sub>3</sub>,” [npj Quantum Materials](#) **3**, 8 (2018).
- <sup>46</sup> Pedro M. C onsoli, Lukas Janssen, Matthias Vojta, and Eric C. Andrade, “Heisenberg-kitaev model in a magnetic field:  $1/s$  expansion,” [Phys. Rev. B](#) **102**, 155134 (2020).
- <sup>47</sup> P. Peter Stavropoulos, Xiaoyu Liu, and Hae-Young Kee, “Magnetic anisotropy in spin-3/2 with heavy ligand in honeycomb mott insulators: Application to cr<sub>2</sub>i<sub>3</sub>,” [Phys. Rev. Research](#) **3**, 013216 (2021).

- <sup>48</sup> Lebing Chen, Jae-Ho Chung, Matthew B. Stone, Alexander I. Kolesnikov, Barry Winn, V. Ovidiu Garlea, Douglas L. Abernathy, Bin Gao, Mathias Augustin, Elton J. G. Santos, and Pengcheng Dai, “Magnetic field effect on topological spin excitations in  $\text{CrI}_3$ ,” *Phys. Rev. X* **11**, 031047 (2021).
- <sup>49</sup> C. Lanczos, “An iteration method for the solution of the eigenvalue problem of linear differential and integral operators,” *Journal of research of the National Bureau of Standards* **45**, 282 (1950).
- <sup>50</sup> Ingo Peschel and Viktor Eisler, *Computational Many-Particle Physics*, edited by H. Fehske, R. Schneider, and A. Weiße, Exact Diagonalization Techniques, Vol. 739 (Springer Berlin Heidelberg, Berlin, Heidelberg, 2008) pp. 529–544.
- <sup>51</sup> S. W. (Stephen W.) Lovesey, *Theory of neutron scattering from condensed matter* (Clarendon Press, 1984).
- <sup>52</sup> T. Holstein and H. Primakoff, “Field Dependence of the Intrinsic Domain Magnetization of a Ferromagnet,” *Physical Review* **58**, 1098 (1940).
- <sup>53</sup> J. H.P. Colpa, “Diagonalization of the quadratic boson hamiltonian,” *Physica A: Statistical Mechanics and its Applications* **93**, 327–353 (1978).

## Acknowledgements

We thank J. Gordon, I. Lee, C. Hammel, S. Nagler, and A. Tennant for useful discussions. This work was supported by the Natural Sciences and Engineering Research Council of Canada and the Canada Research Chairs Program. This research was enabled in part by support provided by Sharcnet ([www.sharcnet.ca](http://www.sharcnet.ca)) and Compute Canada ([www.computecanada.ca](http://www.computecanada.ca)). Computations were performed on the GPC and Niagara supercomputers at the SciNet HPC Consortium. SciNet is funded by: the Canada Foundation for Innovation under the auspices of Compute Canada; the Government of Ontario; Ontario Research Fund - Research Excellence; and the University of Toronto.